Materials Advances

ROYAL SOCIETY OF CHEMISTRY

PAPER

View Article Online
View Journal | View Issue

Cite this: *Mater. Adv.*, 2020, **1**, 918

Luminescent hybrid coatings prepared by a sol–gel process for a textile-based pH sensor

Aicha Boukhriss,[a] Mohamed El messoudi,[ab] Jean-Philippe Roblin,[c] Tarik Aaboub,[ab] Damien Boyer *[c] and Said Gmouh*[b]

Received 16th April 2020,
Accepted 16th June 2020

DOI: 10.1039/d0ma00211a

rsc.li/materials-advances

Fluorene- and stilbene-based fluorophores were synthesized and characterized by NMR, IR, and mass spectroscopy (ESI-MS). These fluorescent dyes were coated onto cotton fabrics by the sol–gel method using tetraethylorthosilicate (TEOS) and propyltriethoxysilane (PTES) as silica precursors. Herein, the optical properties of the synthesized compounds and the elaborated fabrics were studied. The luminescent properties of the fluorophores were examined in three forms: as a powder, dissolved in ethanol, and grafted onto the fabric by the sol–gel method. Furthermore, the effect of the fluorophore concentrations in the sol–gel solution on the fluorescence properties of the elaborated hybrid coatings was investigated. The synthesized fluorophores exhibited good pH sensitivity and a strong wavelength shift in acidic or basic media, ascribed to the protonation–deprotonation of the phenolic groups and pyridine of the fluorophore molecules. Alongside this, we successfully developed pH-sensitive fluorescent textiles and tested their efficiency in different pH media.

1. Introduction

In the last two decades, fluorescent dyes or fluorophores have received considerable attention because of their potential applications, including in traceability, sensing, detection, and labeling targeting molecules.[1–3] These dyes have also been used for the detection of toxic metals,[4,5] traces of explosives,[6,7] and in bio-imaging for the detection of cancer cells or the visualization of living organisms.[8,9] These compounds have shown their ability to be employed as pH sensors and pH probes, due to their high fluorescence quantum yield, and due to their better sensitivity than conventional dyes, such as phenolphthalein and Thymol blue.[10] They are therefore widely used in analytical and bio-analytical chemistry,[11] in cell biology,[12,13] and in medicine.[14]

Fluorophores grafted onto textiles have been used for different applications, such as design, fashion materials, and cloths. Several studies have also reported the immobilization of fluorophores on textiles.[15–17] Indeed, the deposition of fluorescein into cotton yarns using the impregnation method was reported for anti-counterfeiting applications.[18] Khan *et al.*[19] provided a new strategy for the applications of dye molecules on textiles by coating fluorescein isothicyanate-labeled poly(allylamine hydrochloride) and poly(acrylic acid) on cotton fabric by a method involving the layer-by-layer (LbL) assembly of films. Luo *et al.*[20] reported the use of the dip-dyeing process to immobilize the fluorescent material onto cotton fibers to detect and separate the Cd^{2+} in water. The luminescent carbon nanoparticles were prepared by an *in situ* hydrothermal synthesis, and then directly applied to obtain fluorescent cotton fibers. Upon photonic excitation with different wavelengths, the prepared fibers emitted bright and colorful photoluminescence.[21] The application of a lanthanide metal–organic framework to prepare photoluminescent viscose fabrics[22] and to develop photoluminescence cotton fabrics for traffic safety employing a spray-coating approach have also been reported.[23]

The sol–gel method is a technique that can be used to trap molecules, such as fluorophore, in a 2D or 3D silica-based system, and is a technique well known for its low-temperature conditions and its ability to achieve different shapes.[24–28] This process requires hydro-alcoholic solutions of an organometallic precursor, whereby most of the time a hybrid film is coated onto the textile surface to confer it new functionalities, depending on the entrapped molecules, such as flame retardancy,[29] water repellency,[30] or anti-microbial.[31,32] Besides, when a chromic dye is incorporated inside the sol–gel coating, the surface of the textile materials can be used as a pH probe, which leads to flexible sensors that offer the possibility for continuously controlling the pH of large volume systems.[33] Fluorescent dyes can play a similar role with emission spectra that are pH-dependent upon UV excitation. Additionally, these fluorophores must be able to provide a first accurate pH value so that they can be used as very sensitive pH sensors in strips for medical and paramedical uses, for example. The preparation of a textile-based, highly sensitive pH sensor can be also used to determine the pH of

[a] *Laboratory REMTEX, ESITH, Higher School of Textile and Clothing Industries (ESITH), Km 8, Route d'EL JADIDA, Casablanca, Morocco. E-mail: s.gmouh1@gmail.com*
[b] *Laboratory LIMAT, Faculty of Sciences Ben M'Sik, Hassan II University of Casablanca, B.P 5366 Maarif, Casablanca, Morocco*
[c] *Université Clermont Auvergne, CNRS, SIGMA Clermont, Institut de Chimie de Clermont-Ferrand, F-63000 Clermont-Ferrand, France. E-mail: damien.boyer@sigma-clermont.fr*

human sweat, which provides information for patient monitoring and athletes.[34] An example of a textile pH- sensor is the use of branched polymer nanoparticles applied on a polyester conventional textile material by immersing–drying processes.[35] Moreover, the applications of pH-indicator dyes on cotton and nylon were achieved by standard dyeing processes for cotton, and by the electro-spinning process for nylon.[36] Additionally, pH-sensitive polymers based on [poly(acrylic acid)] and [poly(2-vinyl pyridine)] were grafted onto polyester yarns with an epoxide-containing polymer.[37]

As is well known, the fluorescence of quadripolar dyes is strongly sensitive to the pH value in aqueous solution. In this work, we grafted some of these fluorophores based on fluorene and stilbene and bearing at their extremities a phenolic hydroxyl group onto cotton fabrics by the sol–gel process. Efficient pH-induced fluorescence of these smart textiles was expected to be observed.

For this purpose, we synthesized and characterized four fluorophores: 2-(*N*-(4-acetoxystyryl)phenyl)-*N*-ethylamino)ethanol (**P1**), 2-(*N*-(4-(2-(pyridin-4yl)vinyl)phenyl)amino)ethane-1-ol (**P2**), Synthesis of 4-(2-{7-[2(4hydroxy-phenyl)-vinyl]-9,9-dihexyl-9*H*-fluoren-2-yl}-vinyl)-phenyl ester (**P3**) and 4-(2-{7-[2(pyridine)-vinyl]-9,9-dihexyl-9*H*-fluoren-2-yl} -vinyl)-phenylester (**P4**). All the products were analyzed by infrared spectroscopy (IR), nuclear magnetic resonance (NMR) and electrospray ionization-mass spectroscopy (ESI-MS). The optical properties of the synthesized compounds were recorded and are discussed herein. Then, the fluorescent dyes were applied on cotton fabrics by the sol–gel method using tetraethylorthosilicate (TEOS) and propyltriethoxysilane (TPES) as silica precursors, employing the pad–dry–cure technique. The morphology of the coated cotton fabrics with the fluorophore added *via* the sol–gel process was observed by scanning electron microscopy (SEM), and the optical properties of the elaborated fabrics were also investigated. The pH sensitivity of the synthesized fluorophores was studied and pH sensors grafted onto textile materials were designed.

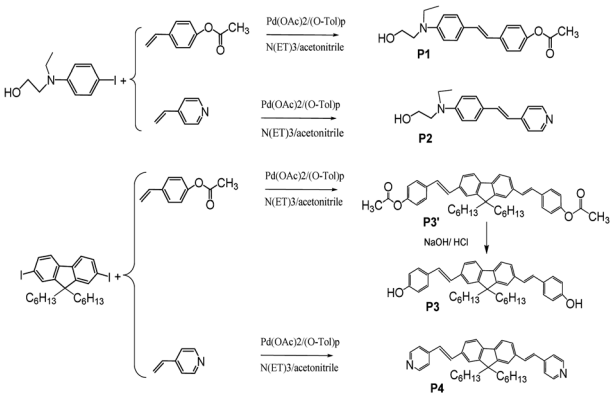

Scheme 1 Synthetic routes to **P1**, **P2**, **P3**, and **P4** fluorophores.

2. Experimental

2.1. Materials and method

Cotton (CO) woven fabric weighing 168 g m^{-2} was used. Tetraethylorthosilicate (TEOS, M_w = 208.33 g mol^{-1}), propyl triethoxysilane (PTES, M_w = 206.35 g mol^{-1}), ethanol (EtOH, 99%), and HCl (37%) were purchased from Sigma-Aldrich and Merck Chemical companies. All the chemicals were analytically pure and used without further purification.

2.1.1. Mass spectrometry. ESI-MS data were obtained on a Quattro II tandem quadrupole mass spectrometer (Micromass, Manchester, UK) fitted with electrospray ionization.

2.1.2. ^{1}H NMR and ^{13}C NMR spectra. ^{1}H NMR and ^{13}C NMR spectra were recorded on Bruker Avance (300 MHz) apparel using TMS as an internal reference. The splitting patterns recorded in this work were: s (singlet), d (doublet), dd (double-of-doublet), t (triplet), p (pentet), and m (multiplet).

2.1.3. Fourier-transform infrared spectroscopy FTIR-ATR. The infrared spectra were recorded on a Nicolet iS10 FTIR-ATR spectrophotometer. The source type was a mid-infrared Ever-Glo and tungsten/halogen. The spectral range for the device was 4000–750 cm^{-1} optimized, with a mid-infrared beamsplitter with a resolution better than 0.4 wavenumbers.

2.1.4. Scanning electron microscopy (SEM). The SEM micrographs were recorded using a ZEISS Supra 55VP scanning electron microscope operating under a high vacuum at 3 kV and using a secondary electron detector (Everhart-Thornley detector).

2.1.5. Photoluminescence measurements. The fluorescence spectra were recorded in dilute solution, using a spectrofluorometer (HAMAMATSU Photonics Multi-Channel Analyzer PMA-12) in the scanning mode from 250 to 500 nm with a step of 5 nm. The excitation source was a 400 W xenon lamp whose wavelength was selected using a Jobin-Yvon TRIAX 180 monochromator equipped with two 600 rpm and 1400 rpm gratings. The fluorescence emitted by the sample was focused on a bundle of optical fibers connected to a Jobin-Yvon TRIAX 550 monochromator equipped with three gratings (150, 1200, and 2400 rpm) and a CCD camera. The SYMPHONY 1024 × 256 pixels was cooled with liquid nitrogen. The entire device was, therefore, suitable for excitation between 200 and 800 nm and detection emission between 250 and 1000 nm.

Quantum yield efficiencies were measured using the C9920-02G PL-QY measurement system from Hamamatsu. The set-up consisted of a 150 W monochromatized Xe lamp, an integrating sphere (Spectralon Coating, ϕ = 3.3 in.), and a high sensitivity CCD camera.

2.2. Synthesis and characterization of the compounds

2.2.1. Synthesis of 2-(*N*-(4-acetoxystyryl)phenyl)-*N*-ethylamino)ethanol (P1). In a flask surmounted by a condenser, 3 g (0.103 mmol) of 2-[ethyl(4-iodophenyl)-amino]ethanol was dissolved in 90 ml of acetonitrile and deaerated by bubbling under argon for 30 min at room temperature. Subsequently, 4.41 g (0.271 mmol) of acetoxystyrene, 39.9 mg (1.77 mmol) of palladium diacetate, 36.4 mg (1.19 mmol) of tri-*o*-polyphosphine, and 2.77 g (0.274 mmol) of triethylamine were added. The solution was heated at 95 °C and left under stirring for 24 h. The residue was purified by using a chromatographic column of silica eluting with a mixture of ethyl acetate/cyclohexane (1 : 1), to obtain a solid brown product. Yield 86.8%, FT-IR (KBr) ν cm^{-1}: 3351 cm^{-1} (ν, OH), 2965–2877 cm^{-1} (ν, CH alkane), 1747 cm^{-1} (ν, C═O), 1600–1500 cm^{-1} (ν, aromatic C═C), 1353 cm^{-1} (ν, CN), 960 (ν, ═C–H). ^{1}H NMR (400 MHz, $CDCl_3$, 298 K): δ (ppm) 1.19(t, 3H), 2.31(s, 3H), 3.47(q, 2H), 3.51(t, 2H),

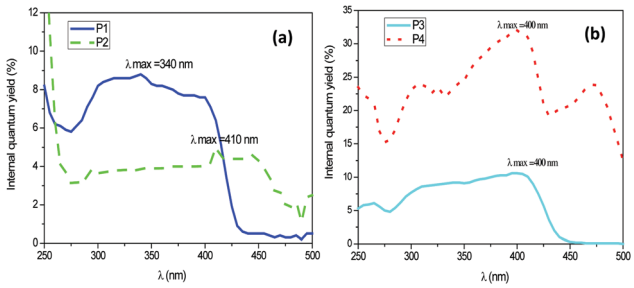

Fig. 1 Internal quantum yield *versus* excitation wavelength for (a) **P1** and **P2**, (b) **P3** and **P4** fluorophores.

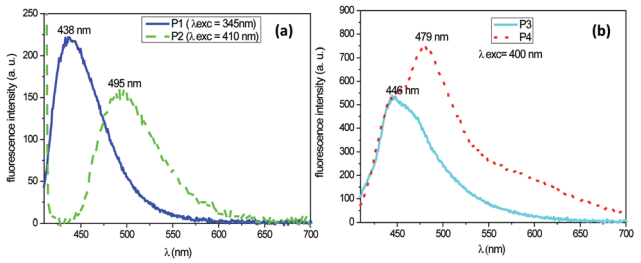

Fig. 2 Emission spectra recorded at RT for (a) **P1** and **P2**, (b) P3 and **P4** fluorophores.

3.82(t, 2H), 6.80(d, 2H, ArH), 6.88–6.92(d, 1H, CH═CH), 6.97–7.01(d, 1H, CH═CH), 7.05–7.08(d, 2H, ArH), 7.40–7.42(d, 2H, ArH), 7.47–7.49(d, 2H, ArH). ^{13}C NMR (400 MHz, $CDCl_3$, 298 K): δ (ppm) 169.55, 149.24, 135.78, 128.65, 127.69, 126.75, 121.54, 59.78, 21.02, 11.76. ESI-MS: *m*/*z* calcd for $C_{20}H_{23}NO_3$ 326 and found 325.

2.2.2. Synthesis of 2-(*N*-(4-(2-(pyridin-4-yl) vinyl) phenyl) amino) ethane-1-ol (P2). In a flask surmounted by a condenser, 3 g (0.103 mmol) of 2-[ethyl (4-iodophenyl) amino] ethanol in 90 ml of acetonitrile was deaerated by bubbling under argon for 30 min at room temperature. Next, 2.48 g (0.235 mmol) of vinylpyridine, 34.2 mg (1.52 mmol) of palladium diacetate, 31.42 mg (1.02 mmol) of tri-*o*-polyphosphine, and 2.38 g (0.235 mmol) of triethylamine were added, and the solution was heated at 95 °C and left under stirring for 24 h. The product was purified by crystallization from acetonitrile to obtain a solid yellowish green product. Yield 72%, FT-IR (KBr) ν cm^{-1}: 3351 cm^{-1} (ν, OH), 2965–2877 cm^{-1} (ν, CH alkane), 3259 cm^{-1} (ν, OH), 2957–2862 cm^{-1} (ν, CH alkane), 1517–1464 cm^{-1} (ν, C═C aromatic), 964 cm^{-1} (ν, ═C–H vinyl). ^{1}H NMR (400 MHz, $CDCl_3$, 298 K): δ (ppm) 1.19(t, 3H), 3.47(q, 2H), 3.52(t, 2H), 3.83(t, 2H), 6.7–6.72(d, 1H, CH═CH), 6.75–6.79(d, 1H, CH═CH), 7.22–7.26(d, 2H, ArH), 7.30–7.31(d, 2H, ArH), 7.38–7.40(d, 2H, ArH), 8.45–8.46(d, 2H, ArH) ^{13}C NMR (400 MHz, $CDCl_3$, 298 K): δ (ppm) 149, 133.69, 128.62, 123.81, 120.44, 112.03, 77.32, 76.68, 59.90, 52.32, 45.48, 30, 88.11, 94. ESI-MS: *m*/*z* calcd for $C_{17}H_{20}N_{2O}$ 269 and found 269.

2.2.3. Synthesis of 4-(2-{7-[2(4hydroxy-phenyl)-vinyl]-9,9-dihexyl 9*H*-fluoren-2-yl}-vinyl)-phenyl ester (P3). In a flask surmounted by a condenser, 3 g (5.11 mmol) of 9,9-dihexyl-2,7-diiodo-9*H* fluorene in 90 ml of acetonitrile was deaerated by bubbling under argon for 30 min at 25 °C. Next, 1.65 g (1.022 mmol) of acetoxystyrene, 57 mg (0.255 mmol) of palladium diacetate, 155 mg (0.511 mmol) of tri-*o*-polyphosphine, and 1.18 g (11.7 mmol) of triethylamine were added. The solution was heated at 95 °C and left under stirring for 24 h, and the solvent was then removed under vacuum using a rotary evaporator. Next, a solution of 5 ml of NaOH (1 M) in 10 ml of EtOH was added dropwise and the reaction medium was stirred for 2 h. Afterwards, a solution of HCl (1 M) was added to the mixture until a neutral pH was reached. The product was then extracted with CH_2Cl_2. The residue was purified in a column of silica using CH_2Cl_2/cyclohexane (1/1) as the eluent and then the column was terminated with ethyl acetate t0 obtain a solid brown product. Yield 27%, FT-IR (KBr) ν cm^{-1}: 3301 cm^{-1} (ν, OH), 2919–2850 cm^{-1}(ν, CH aliphatique), 1408–1442 cm^{-1}(ν, C═C aromatic), 956 (ν, ═CH vinyl). ^{1}H NMR (400 MHz, $CDCl_3$, 298 K): δ (ppm) 0.68 (s, 4H, CH_2), 0.77(t, 6H, CH_3), 1.13–1.06(m, 12H, CH_3), 2(m, 4H, CH_2), 6.85–6.87(d, 4H), 7.10–7.08(d, 2H), 7.44–7.46(d, 8H), 7.48(s, 2H) 7.66–7.64(d, 2H). ^{13}C NMR (400 MHz, $CDCl_3$, 298 K): δ (ppm) 155.05, 151.09, 143.03, 139.94, 136.09, 132.02, 129.90, 127.45, 126.77, 120.08, 115.37, 110.29, 108.93, 54.55, 40.20, 31.12, 29.38, 23.39, 22.23, 21.65, 13.65 ESI-MS: *m*/*z* calcd for $C_{41}H_{46}O_2$ 570.82 and found 586.

2.2.4. Synthesis of 4-(2-{7-[2-(pyridine)-vinyl]-9,9-dihexyl-9*H*-fluoren-2-yl}-vinyl)-phenyl ester (P4). In a flask surmounted by a condenser, 1 g (1.7 mmol) of 9,9-dihexyl-2,7-diiodo-9*H* fluorene in 30 ml of acetonitrile was deaerated by bubbling under argon for 30 min at room temperature. Next, 0.358 g (3.41 mmol) of vinylpyridine, 57.2 mg (0.085 mmol) of palladium diacetate, 51.7 mg (0.17 mmol) of tri-*o*-polyphosphine, and 34.5 mg (3.41 mmol) of triethylamine were added, and the solution was heated at 95 °C and left under stirring for 24 h. The residue was purified in a column of silica using CH_2Cl_2/heptane (1/1) as eluent to obtain a solid green product. Yield 30%, ^{1}H NMR (400 MHz, $CDCl_3$, 298 K): δ (ppm) 0.65(s, 4H, CH_2), 0.75(t, 6H, CH_3), 1.02–1.08(m, 12H, CH_3), 2(m, 4H, CH_2), 7.07–7.11(d, 2H), 7.10–7.08(d, 2H), 7.40–7.44(d, 4H), 7.52–7.56(d, 6H) 7.71–7.72(d, 2H). 8.5–8.60(d, 4H). ^{13}C NMR (400 MHz, $CDCl_3$, 298 K): δ (ppm) 151.84, 149.86, 145.13, 141.52, 135.38, 133.99, 126.46, 125.27, 121.35, 120.88, 120.34, 55.17, 40.50, 31.52, 29.72, 23.79, 22.60, and 14.03. ESI-MS: *m*/*z* calcd for $C_{39}H_{44}N_2$ 540.79 and found 541.

Table 1 Fluorescence data for **P1**, **P2**, **P3**, and **P4** fluorophores

	Fluorescence data			
Fluorophore	$\lambda_{max\,ex}$ (nm)	$\lambda_{max\,em}$ (nm)	Φ_i [%]	Φ_a [%]
P1	340	438	8.7	8.5
P2	410	495	5.0	4.9
P3	400	446	10.6	10.4
P4	400	479	32.0	31.6

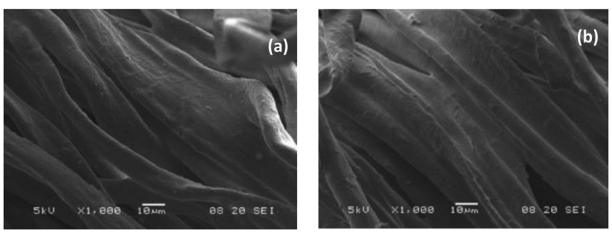

Fig. 3 SEM images of the cotton fibers for samples (a) T3 and (b) T4.

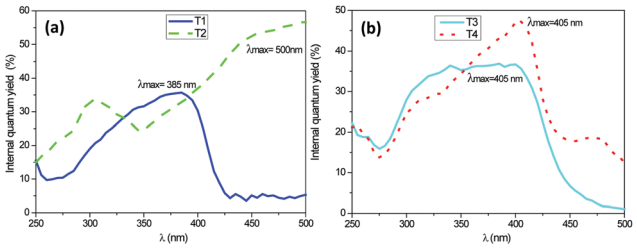

Fig. 4 Internal quantum yield *vs.* excitation wavelength for (a) T1 and T2, (b) T3 and T4.

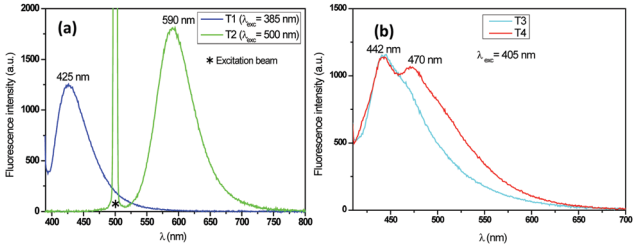

Fig. 5 Fluorescence emission spectra of (a) T1 and T2 and (b) T3 and T4 fabrics.

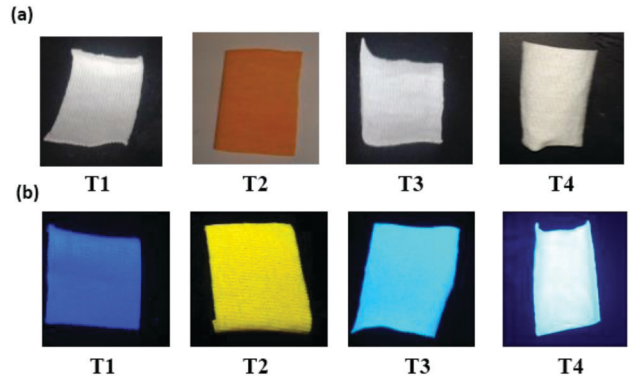

Fig. 6 Sol–gel-treated fabrics (a) upon daylight exposure and (b) upon UV excitation at 365 nm.

2.3. Preparation of the hybrid coatings by the sol–gel process

Cotton fabrics were coated using the sol–gel process combined with the pad–dry–cure technique. TEOS (50%)/PTES (50%), HCl (0.01 M), distilled water, and EtOH were mixed with a molar ratio of 10/0.008/60/55 to obtain the sol–gel solution. The fluorescent dyes were added to give a concentration corresponding to 1.05 mmol L^{-1}. The solution was agitated for 3 h at 70 °C. Then, the cotton fabrics were impregnated in the solution and padded to give 80% weight pick-up. The samples were dried for 30 min at 80 °C and cured for 1 h at 120 °C. The resulting fabrics coated with the fluorophores *via* the sol–gel process were respectively labeled T1, T2, T3, and T4.

Table 2 Solutions and sols prepared with different fluorophore concentrations

Fluorophore	Concentration in solution (mol L^{-1})		Concentration in sol (mol L^{-1})
P3, P4	C1	1.05×10^{-3}	1.05×10^{-3}
P3, P4	C2	2.1×10^{-4}	2.1×10^{-4}
P3, P4	C3	1.48×10^{-4}	1.48×10^{-4}
P3, P4	C4	1.05×10^{-4}	1.05×10^{-4}
P3, P4	C5	2.79×10^{-5}	2.79×10^{-5}
P3, P4	C6	9.32×10^{-6}	9.32×10^{-6}
P3, P4	C7	1.05×10^{-6}	1.05×10^{-6}

3. Results and discussion

3.1. Fluorophores synthesis

In this study, four organic fluorophores were obtained *via* the Mizoroki–Heck coupling between fluorene and stilbene cores substituted with two different arms, as depicted in Scheme 1. The fluorophores were characterized and their molecular structures were confirmed by FT-IR, ^{1}H NMR, and ^{13}C NMR analysis and mass spectroscopy.

3.2. Optical properties of the fluorophores in solution

The internal quantum yield curves as a function of the excitation wavelength of the synthesized fluorophores (**P1**, **P2**, **P3**, and **P4**) are gathered in Fig. 1. These measurements were carried out with dilute solutions of ethanol. The fluorescent dyes concentrations were about 1.05 mmol L^{-1}. We noted the internal quantum yields by Φ_i (number of photons emitted) and the absolute quantum yields by Φ_a ($\Phi_a = \Phi_i$* absorbance).

According to this figure, the maximum excitation wavelength of **P1** and **P2** based on stilbene fluorophores was respectively 340 nm and 410 nm, whereas it was 400 nm for the quadripolar fluorophores **P3** and **P4**. The emission spectra of the four fluorescent dyes were recorded upon excitation at these different wavelengths at 300 K.

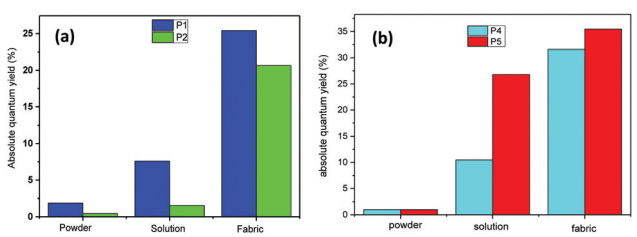

Fig. 7 Absolute quantum yields in different types of samples for (a) **P1**, **P2** fluorophores and (b) **P3**, **P4** fluorophores.

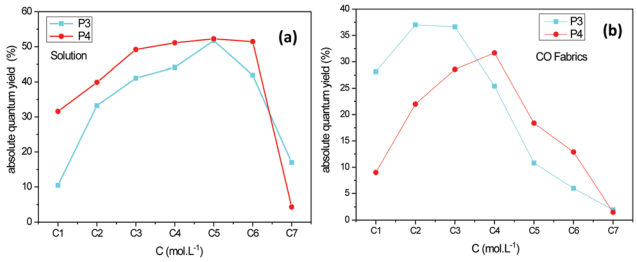

Fig. 8 Absolute quantum yield as a function of the concentration (a) in solution and (b) on the coated CO fabrics for **P3** and **P4** fluorophores.

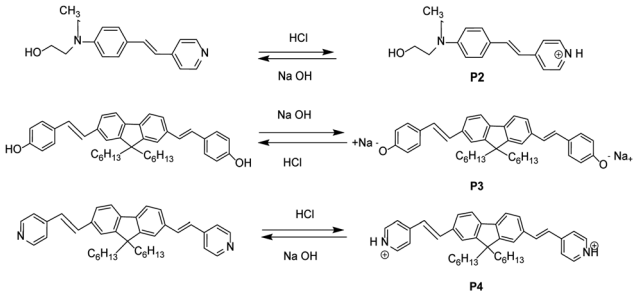

Scheme 2 Protonation and deprotonation forms of the **P2**, **P3**, and **P4** fluorophores.

Table 1 summarizes all the fluorescence data for each of them. The absolute quantum yields were added in this table, considering that the absorption was nearly 100% for each fluorophore at their maximum excitation. Fig. 2a shows that for the fluorophores derived from stilbene, the two compounds **P1** and **P2**, exhibited a strong emission in the blue wavelength range. The fluorophore **P1** bears electron acceptor carbonyl groups, whereas the fluorophore **P2** contains nitrogen atoms, which are very good electron donors, which explain why a bathochromic displacement of 57 nm was observed between the emission spectra of both fluorescent dyes. Similarly, from Fig. 2b, it is observed that the fluorophore **P3** gives rise to a single emission band, while compound **P4** has two main emission bands also in the blue range. The observed bathochromic effect was due to the electro-donor character of the nitrogen, which was stronger than that of the OH groups.

The extension of the π-electron system of the fluorene–core fluorophores compared to those of the stilbene–core was accompanied by increases in the quantum yields of 32% for **P4** and 5% for **P2**.[38]

3.3. Characterization of the treated fabrics

3.3.1. SEM characterization. Fig. 3 shows the SEM images of samples T3 and T4. The coating with the TEOS/PTES mixture was highly homogeneous.[28] It can, therefore, be deduced that the dispersion of the fluorophores in the TEOS/PTES mixture did not affect the polymerization of the alkoxysilanes to achieve high-quality hybrid coatings. Indeed, for all the fluorophores, the coatings were highly homogeneous and well covered the surface of the fibers.

3.3.2. Optical characterization of fabrics coated with the fluorescent hybrid materials. The internal quantum yield curves as a function of the excitation wavelength of the fabrics (T1, T2, T3, and T4) coated with the sols containing the **P1**, **P2**, **P3**, and **P4** fluorophores are shown in Fig. 4.

According to this figure, the maximum excitation wavelength of the fabrics T1, T2, T3, and T4 was 385, 500, and 405 nm, respectively. The emission spectra of the fabrics retained the same profile as those of the solutions previously reported, except for the sample T2, which exhibited a significant bathochromic shift of 95 nm (Fig. 5). This bathochromic displacement was mainly due to the presence of HCl traces used as a catalyst for the preparation of the sol–gel solution. These results were visually confirmed by comparing the luminescent hybrid coated fabrics upon daylight exposure and upon 365 nm irradiation with a UV lamp as shown in the pictures in Fig. 6. For all the fabrics except T2, the fluorophores were colorless upon daylight exposure (Fig. 6a), whereas upon UV excitation, the fabrics emitted fluorescence with different colors (Fig. 6b).

In order to investigate the effect of the sol–gel coating on the luminescent properties of the fluorophores, these latter materials were examined in three forms: as a powder, dissolved in ethanol, and grafted onto the fabric by the sol–gel method. The quantum yields of the fluorophores in the different forms are presented in Fig. 7. The fluorophores powder did not emit fluorescence, which can be explained by the absence of the dispersive medium and thus by a concentration quenching effect since the molecules are too close to each other. When they are grafted to the surface of textiles, their quantum efficiency is even higher than dissolved in the solution. This is certainly due to the presence of silica, which disperses the fluorophore molecules, thus playing the role of a solid solvent. The bathochromic effect observed for the fluorophore **P2** was attributed to the protonation of pyridine by HCl used during the sol–gel synthesis.

3.3.3. Effect of the fluorescent dyes concentration on the optical properties. We only performed this study for the **P3** and **P4** fluorophores since they exhibited a higher quantum yield. We started by preparing several solutions with different fluorophore concentrations with the aim to measure their quantum yield. Similarly, we prepared several sol–gel solutions (50%TEOS/50% PTES) with different concentrations for the purpose to coat them onto cotton fabrics. All the relevant information is gathered in Table 2.

From Fig. 8, it can be observed that the absolute quantum yield of fluorescence goes to a maximum. Also, it is noticeable that the emission intensity decreased when the concentration of the solutions increased. The maximum absolute quantum yields of the **P3** and **P4** fluorophores was 52% in the solution for the concentrations

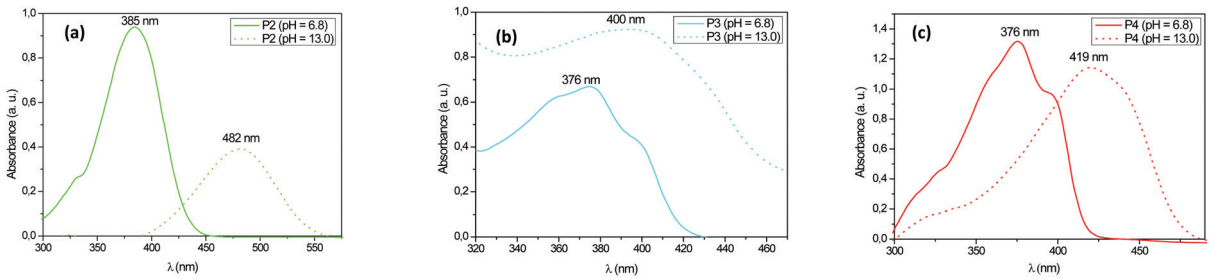

Fig. 9 Absorption spectra of the protonated and deprotonated forms of (a) **P2**, (b) **P3**, and (c) **P4** fluorophores in solution.

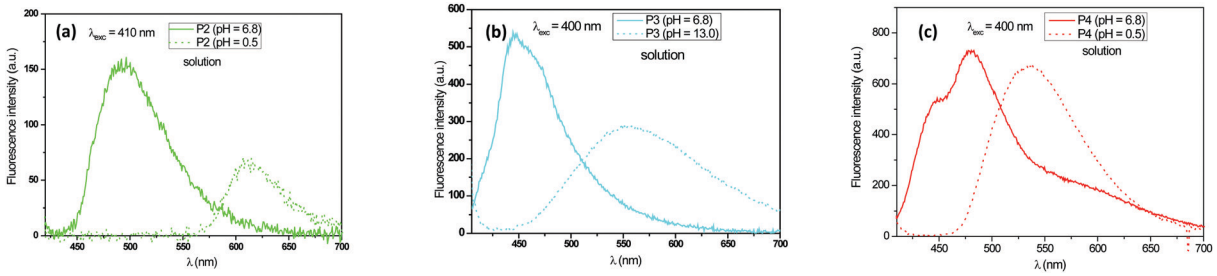

Fig. 10 Emission spectra as a function of pH for the (a) **P2**, (b) **P3**, and (c) **P4** fluorophores in solution.

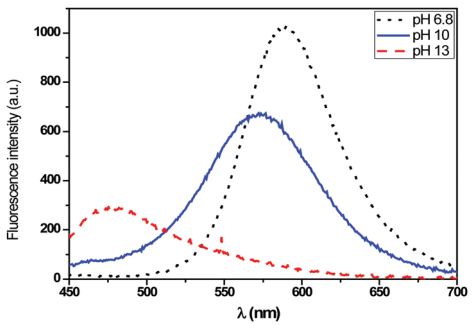

Fig. 11 Emission spectrum of the T2 fabric as a function of pH upon excitation at 400 nm.

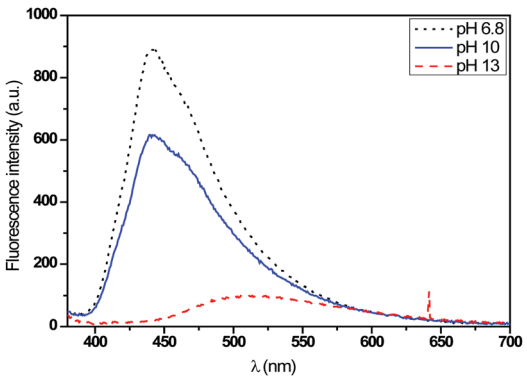

Fig. 13 Emission spectrum of the T3 fabric as a function of pH under excitation at 365 nm.

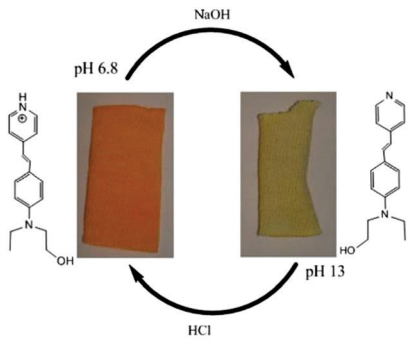

Fig. 12 Schematic of the fabricated textile as a pH sensor/orange-yellow halochromic material.

between C5 and C6. The same trend was observed in the case of the grafted fabrics, where the maximum absolute quantum yield was 37% for **P3** and 31% for **P4** for concentrations between C2 and C3. We can conclude that with a small quantity of fluorophore dispersed on the surface of the textile we can achieve suitable luminescent properties, thus allowing us to develop a tracer or pH-sensitive textile strip.

3.4. Development of a pH sensor

3.4.1. pH-Sensitive properties in aqueous solution. To exploit the pH sensory abilities of the synthesized fluorophores, we studied the peculiar optical properties associated with their protonated (acidic) and deprotonated (basic) form. The protonation and deprotonation forms of the synthesized fluorophores **P2**, **P3**, and **P4** by HCl and NaOH solutions are shown in Scheme 2. It is worth noting that **P1** did not exhibit protonated and deprotonated species.

The absorption properties of these fluorophores were modified with the change in the concentration of hydronium ions (pH). As shown in Fig. 9, the **P2** and **P4** fluorophores went through a bathochromic shift, over 95 nm for the fluorophore **P2** and more than 40 nm for the fluorophore **P4** as observed when the pH value decreased, while the **P3** fluorophore led to a slight bathochromic shift along with an increase of the absorbance intensity when the pH was increased from 6.8 to 13. We assume that the pH dependence of the absorption intensities on the UV-visible spectra was directly linked to the protonation–deprotonation of the fluorophores and thus the presence in solution of their acidic or basic species.

To evidence their pH sensitivity, the emission spectra of each fluorescent dyes were recorded in solution at different pH upon excitation at their optimal wavelength. The results, shown in Fig. 10, undoubtedly indicated their ability to be used as pH sensors.

3.4.2. pH-Sensor properties on cotton fabrics. Textile-based pH sensors T2, T3, and T4 were prepared using the previous **P2**, **P3**, and **P4** fluorescent dyes incorporated in sol–gel solutions and coated onto cotton fabrics by the pad–dry–cure technique. With the aim to demonstrate the effectiveness of these sensors, the samples were immersed separately in solutions with an experimentally measured pH of 0.5, 6.8, 10.0, and 13.0, and then their optical properties were recorded and compared.

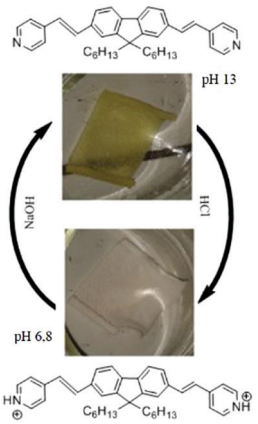

Fig. 14 Schematic of fabricated textile as a pH sensor/invisible-yellow halochromic material.

For the T2 sample, the main emission band was shifted from the orange wavelength range to the yellow-green one while turning the pH from neutral to basic (Fig. 11 and 12), which may be explained by the change from the protonated form to the deprotonated form. The orange fluorescence of the textile was due to the protonation of the pyridine arm by the HCl added during the preparation of the sol. The passage to the basic medium was also accompanied by the change of color from orange to yellow and a decrease in fluorescence, as shown in the Fig. 11 and 12.

As shown in Fig. 13 and 14, the fluorescence spectrum of the T3 fabric changed from an emitting band in the blue range to weak green emission when the pH changed from neutral to basic, which corresponds to the protonation–deprotonation mechanism of the fluorophore molecule. The transition to the base medium was also accompanied by a change in color from transparent to yellow.

In Fig. 15, a decrease of the fluorescence intensity was also observed when the pH values increased. In the case of the T4 fabric, the emission spectrum switched from a broad blue light to an emission in the green range when the fabric was immersed in acidic medium. The immersion of the fabric in the basic medium caused no shift in the emission spectrum. Here, we understand that the acid added during the synthesis of the sols was not sufficient enough to carry out the total protonation of the two pyridine arms.

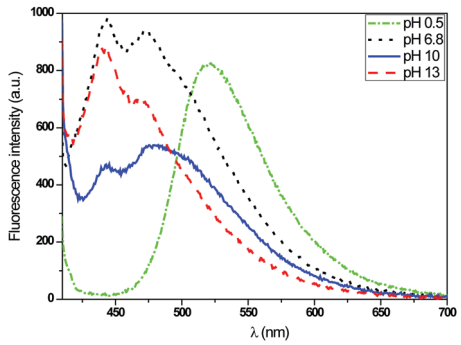

Fig. 15 Emission spectra of the T4 fabric as a function of pH under excitation at 400 nm.

4. Conclusion

Regarding this work, we started with the synthesis of different organic fluorophores using the Heck coupling of stilbene and fluorene cores. All the obtained compounds had excellent solubility in organic and inorganic solvents, especially in ethanol. Their photoluminescence properties were recorded, notably, the excitation and emission spectra. These fluorophores were grafted onto textile surfaces using the sol–gel process and employing the pad–dry–cure method. The emission spectra confirmed their grafting on textile surfaces with relatively high absolute fluorescence yields. The optical properties of the fluorophores in powder form, in solution, and grafted onto the fabric were assessed and discussed. The effect of the fluorophore concentrations used for the sol–gel method on the photoluminescent properties of the elaborated fabrics was also investigated in this work. Finally, we successfully developed a pH-sensitive fluorescent textiles sensor by the protonation and deprotonation of the phenolic groups and pyridine of the synthesized fluorophores and we evidenced its effectiveness.

Conflicts of interest

There are no conflicts to declare.

References

1 Y.-Y. Guo, L.-Z. Yang, J.-X. Ru, X. Yao, J. Wu, W. Dou, W.-W. Qin, G.-L. Zhang, X.-L. Tang and W.-S. Liu, *Dyes Pigm.*, 2013, **99**, 693–698.
2 L. Yang, W. Yang, D. Xu, Z. Zhang and A. Liu, *Dyes Pigm.*, 2013, **97**, 168–174.
3 N. Fu, Y. Chen, J. Fan, G. Wang and S. Lin, *Sens. Actuators, B*, 2014, **203**, 435–443.
4 I. Leray and B. Valeur, *Eur. J. Inorg. Chem.*, 2009, 3525–3535.
5 T. Balaji, S. A. El-Safty, H. Matsunaga, T. Hanaoka and F. Mizukami, *Angew. Chem., Int. Ed.*, 2006, **45**, 7202–7208.
6 R. Tu, B. Liu, Z. Wang, D. Gao, F. Wang, Q. Fang and Z. Zhang, *Anal. Chem.*, 2008, **80**, 3458–3465.
7 X. Wang, Y. Guo, D. Li, H. Chen and R. Sun, *Chem. Commun.*, 2012, **48**, 5569–5571.
8 T. R. Krishna, M. Parent, M. H. V. Werts, L. Moreaux, S. Gmouh, S. Charpak, A.-M. Caminade, J.-P. Majoral and M. Blanchard-Desce, *Angew. Chem., Int. Ed.*, 2006, **45**, 4645–4648.
9 Y. Kimura, A. Momotake, N. Takahashi, H. Kasai and T. Arai, *Chem. Lett.*, 2012, **41**, 528–530.
10 D. Staneva and R. Betcheva, *Dyes Pigm.*, 2007, **74**, 148–153.
11 M. F. Frasco and N. Chaniotakis, *Anal. Bioanal. Chem.*, 2010, **396**, 229–240.
12 J. Zhang, R. E. Campbell, A. Y. Ting and R. Y. Tsien, *Nat. Rev. Mol. Cell Biol.*, 2002, **3**, 906–918.
13 D. W. Domaille, E. L. Que and C. J. Chang, *Nat. Chem. Biol.*, 2008, **4**, 168–175.
14 W. W. Miller, M. Yafuso, C. F. Yan, H. K. Hui and S. Arick, *Clin. Chem.*, 1987, **33**, 1538–1542.
15 G. J. Mohr, *Sens. Actuators, B*, 2018, **275**, 439–445.

16 D. Staneva, E. Vasileva-Tonkova and I. Grabchev, *J. Photochem. Photobiol., A*, 2019, **375**, 24–29.
17 D. Staneva, R. Betcheva and J.-M. Chovelon, *J. Appl. Polym. Sci.*, 2007, **106**, 1950–1956.
18 K. Baatout, F. Saad, A. Baffoun, B. Mahltig, D. Kreher, N. Jaballah and M. Majdoub, *Mater. Chem. Phys.*, 2019, **234**, 304–310.
19 F. Khan, P. Liu, S. Yang, Y. Ma and Y. Qiu, *Dyes Pigm.*, 2017, **142**, 358–364.
20 Y. Luo, D. Tang, W. Zhu, Y. Xu and X. Qian, *J. Mater. Chem. C*, 2015, **3**, 8485–8489.
21 Y. Yu, J. Wang, J. Wang, J. Li, Y. Zhu, X. Li, X. Song and M. Ge, *Cellulose*, 2017, **24**, 1669–1677.
22 H. E. Emam, H. N. Abdelhamid and R. M. Abdelhameed, *Dyes Pigm.*, 2018, **159**, 491–498.
23 T. A. Khattab, M. M. G. Fouda, M. S. Abdelrahman, S. I. Othman, M. Bin-Jumah, M. A. Alqaraawi, H. Al Fassam and A. A. Allam, *J. Fluoresc.*, 2019, **29**, 703–710.
24 A. Bentis, A. Boukhriss, A. M. Grancaric, M. El Bouchti, M. El Achaby and S. Gmouh, *Cellulose*, 2019, **26**, 2139–2153.
25 A. Boukhriss, D. Boyer, H. Hannache, J.-P. Roblin, R. Mahiou, O. Cherkaoui, S. Therias and S. Gmouh, *Cellulose*, 2015, **22**, 1415–1425.
26 A. Boukhriss, S. Gmouh, H. Hannach, J.-P. Roblin, O. Cherkaoui and D. Boyer, *Cellulose*, 2016, 3355–3364.
27 A. Bentis, A. Boukhriss, D. Boyer and S. Gmouh, *IOP Conf. Ser.: Mater. Sci. Eng.*, 2017, **254**, 122001.
28 M. El messoudi, A. Boukhriss, O. Cherkaoui, M. El Kouali and S. Gmouh, *J. Coat. Technol. Res.*, 2019, 1–10.
29 D. Lin, X. Zeng, H. Li, X. Lai and T. Wu, *J. Colloid Interface Sci.*, 2019, **533**, 198–206.
30 B. Wang, B. Lei, Y. Tang, D. Xiang, H. Li, Q. Ma, C. Zhao and Y. Li, *J. Coat. Technol. Res.*, 2018, **15**, 611–621.
31 A. Vilčnik, I. Jerman, A. Šurca Vuk, M. Koželj, B. Orel, B. Tomšič, B. Simončič and J. Kovač, *Langmuir*, 2009, **25**, 5869–5880.
32 J. Vasiljević, M. Zorko, D. Štular, B. Tomšič, I. Jerman, B. Orel, J. Medved, J. Kovač and B. Simončič, *Cellulose*, 2017, **24**, 1511–1528.
33 L. Van der Schueren, K. De Clerck, G. Brancatelli, G. Rosace, E. Van Damme and W. De Vos, *Sens. Actuators, B*, 2012, **162**, 27–34.
34 M. L. Zamora, J. M. Dominguez, R. M. Trujillo, C. B. Goy, M. A. Sánchez and R. E. Madrid, *Sens. Actuators, B*, 2018, **260**, 601–608.
35 J. Jia, K. Chen, T. Zeng, D. Yao and C. Wang, *Ind. Eng. Chem. Res.*, 2020, **59**, 2899–2907.
36 L. Van der Schueren and K. De Clerck, *Int. J. Clothing Sci. Technol.*, 2011, **23**, 269–274.
37 F. Vatansever, R. Burtovyy, B. Zdyrko, K. Ramaratnam, T. Andrukh, S. Minko, J. R. Owens, K. G. Kornev and I. Luzinov, *ACS Appl. Mater. Interfaces*, 2012, **4**, 4541–4548.
38 B. Valeur, *Invitation à la fluorescence moléculaire*, De Boeck supérieur, 2004 Sep 6, ISBN 2804145972.